Asian Journal of Current Research in Clinical Cancer
ISSN: 3062-4444
2025, Volume 5, Issue 2, Page No: 158-167

Available online at: www.galaxypub.co/page/journals

Galaxy Publication

Galaxy Publication

Quantitative NGS with Synthetic Standards for Precise ctDNA Copy Number Assessment in Non-Small Cell Lung Cancer

Y. El Amrani[1*], M. Benali[1], N. El Idrissi[1]

[1]Department of Oncology, School of Medicine, University of Rabat, Rabat, Morocco.

***E-mail** ✉ rabat.onc.40@gmail.com

Received: 03 September 2025; **Revised:** 28 November 2025; **Accepted:** 04 December 2025

ABSTRACT

Analysis of circulating tumor DNA (ctDNA) offers a non-invasive means to track tumor dynamics and treatment response. Reliable quantification approaches are essential to leverage ctDNA as a biomarker for cancer monitoring. While digital PCR (dPCR) provides high precision and sensitivity, it requires prior identification of tumor-specific mutations. Conversely, next-generation sequencing (NGS) offers broader genomic coverage but is semi-quantitative, relying on variant allelic fraction (VAF), which can be confounded by cell-free DNA of non-tumor origin. We established a new quantitative NGS (qNGS) platform that allows absolute measurement of nucleotide variants. The system integrates unique molecular identifiers (UMIs) and quantification standards (QSs) — short synthetic DNA molecules engineered with distinct mutations to be uniquely identifiable in sequencing reads. The method's accuracy was tested using plasma samples spiked with mutant DNA and pooled plasma from cancer patients, and further validated on samples from four non-small cell lung cancer (NSCLC) participants in the ELUCID trial. The qNGS assay exhibited excellent linearity and strong correlation with dPCR results for both experimental and patient plasma samples. In the ELUCID trial samples, the approach successfully quantified multiple variants simultaneously within individual plasma specimens. ctDNA concentrations differed significantly between baseline and post-therapy samples collected three weeks after the start of treatment. This study introduces a qNGS technique enabling absolute ctDNA quantification, unaffected by fluctuations in non-tumor cell-free DNA. Its application to serial NSCLC samples demonstrated simultaneous tracking of multiple mutations, highlighting qNGS as a reliable and versatile tool for precision oncology.

Keywords: ctDNA, Quantification, NGS, dPCR, NSCLC

How to Cite This Article: El Amrani Y, Benali M, El Idrissi N. Quantitative NGS with Synthetic Standards for Precise ctDNA Copy Number Assessment in Non-Small Cell Lung Cancer. Asian J Curr Res Clin Cancer. 2025;5(2):158-67. https://doi.org/10.51847/y01ygb3ZZx

Introduction

Monitoring tumor load is a vital component of cancer management, guiding treatment strategies and supporting individualized therapy. Circulating tumor DNA (ctDNA)—a tumor-derived portion of plasma cell-free DNA—has emerged as a minimally invasive biomarker for this purpose [1]. ctDNA carries the same genetic and epigenetic signatures as the tumor itself, and numerous studies have demonstrated that ctDNA levels closely reflect tumor dynamics, often detecting disease progression earlier than imaging or clinical assessments [2-4]. Moreover, ctDNA profiling aids in understanding tumor evolution and clonal diversity during therapy [5-7].

The clinical effectiveness of ctDNA monitoring depends on accurate quantification, typically achieved via dPCR or NGS. Yet, a standardized approach remains lacking.

In digital PCR, DNA samples are subdivided into numerous small reactions, allowing detection of even single-molecule targets. This enables absolute quantification of mutated DNA copies per milliliter of plasma. Although exceptionally sensitive, the technique is mutation-specific, requiring prior knowledge of the genetic alteration, and thus limits detection to predefined mutations.

NGS, in contrast, allows broad mutation profiling without such prior information. This makes it suitable for patients whose tumors have not been fully genetically characterized. However, NGS-based quantification depends

on VAF, representing the proportion of mutated alleles within total cfDNA. Because total cfDNA levels fluctuate under physiological or pathological conditions—such as infection, inflammation, or stress—VAF measurements may inaccurately estimate tumor burden. Additionally, multiple sample preparation steps (amplification, purification, dilution) can introduce bias, leading to over- or under-representation of DNA molecules and complicating absolute quantification [8-13].

To address these challenges, we created a quantitative NGS (qNGS) strategy that merges the breadth of NGS with absolute quantification expressed as copies per milliliter of plasma. By incorporating UMIs and QSs, this approach minimizes sequencing bias and improves measurement precision for ctDNA monitoring in clinical settings.

UMIs are random DNA tags (8-16 nucleotides) added to each molecule during library preparation, uniquely labeling every original DNA fragment. Even after amplification, sequences sharing the same UMI can be traced back to their source molecule [14], enabling an accurate molecular count prior to amplification.

Nonetheless, some DNA molecules are inevitably lost through extraction, purification, or dilution steps. To compensate, we designed QSs—synthetic 190 bp DNA fragments resembling apoptotic cfDNA in size [15]. Each QS represents a reference genomic locus but contains a distinctive synthetic mutation for identification in sequencing output **(Figure 1)**. A defined concentration of QSs is spiked into plasma before cfDNA extraction, then sequenced using a targeted NGS panel detecting both native reference and QS regions. Because both are sequenced with comparable efficiency, counting QS reads and UMI-labeled native molecules allows accurate estimation of the absolute ctDNA concentration in plasma.

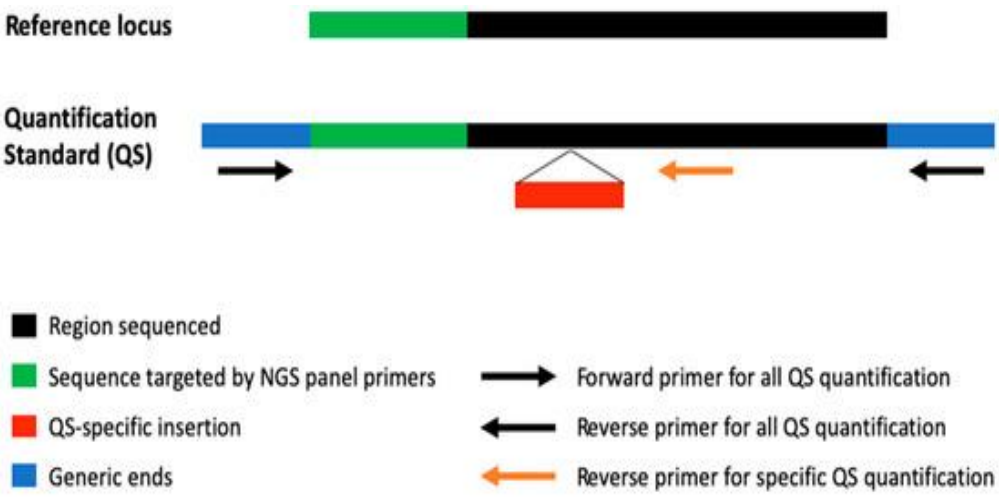

Figure 1. Diagram of the quantification standards (QS). Each QS is built around a 103-bp reference locus, with a distinct 25-bp sequence inserted adjacent to the NGS target region to differentiate QS sequences from endogenous DNA. Generic terminal sequences were added for standardized quantification.

This study evaluates the utility of qNGS for absolute measurement of nucleotide variants in ctDNA, offering a precise and reliable approach to overcome typical analytical challenges in ctDNA quantification.

Materials and Methods

Quantification standards

QS construction

Three QS constructs were designed. Each QS was based on a 103-bp genomic segment from the GRCh38 (hg38) human reference genome.

To differentiate QSs from native sequences, the following modifications were made:

- Insertion of a unique sequence: A 25-bp sequence (GATTACAACACGAGTTCGACCGCGT) was placed near the NGS-targeted region to allow unambiguous identification.
- Generic terminal sequences: Identical 5′ and 3′ sequences were appended to all QSs to permit consistent amplification with a universal primer set. The 5′ end contains a 30-bp sequence

(GTGACATCTACGGTGATCCGACATCTCCTG), and the 3′ end a 32-bp sequence (GTTGTTAGCATCGCCGTCATATCGCAAGGCAT).

The inserted and flanking sequences were chosen arbitrarily, and uniqueness in the human genome was verified via BLAST (https://blast.ncbi.nlm.nih.gov/Blast.cgi, accessed 24 January 2022).

Each QS (total 190 bp) was synthesized as a linear double-stranded DNA fragment using Invitrogen GenArt Strings technology (ThermoFisher, Montigny-le-Bretonneux, France) and rehydrated in water for use.

QS quantification

Absolute copy numbers for each QS were measured using digital PCR (dPCR) on a Naica system (Stilla Technologies, Villejuif, France). A universal primer pair targeting the QS generic ends (Forward: GGTGATCCGACATCTCCTG; Reverse: ATGACGGCGATGCTAACAAC) and a probe complementary to the 25-bp insertion (HEX-GATTACAACACGAGTTCGACCGCG-TAMRA) enabled quantification of all QSs using a single assay.

QSs were diluted to equal concentrations, pooled, and split into 100 µL aliquots stored at −20 °C. To determine precise copy numbers in the pool, triplicate QS-specific dPCR reactions were performed using the universal forward primer, a labeled probe, and QS-specific reverse primers:

- QS1: AGACAGCAGATACTTGATTGGT
- QS2: TCAATGGCTGAGGTGAGGTA
- QS3: CCGTGCCTAGCTCAAACCTA

Plasma spiking and cfDNA extraction

For each sample, 10 µL of the QS pool (containing 18, 000 copies of each QS) was added to 2 mL plasma before lysis. cfDNA was extracted using the Maxwell RSC ccfDNA LV Plasma Kit (Promega, Charbonnières-les-Bains, France) per manufacturer instructions. Extracted DNA was eluted in 60 µL buffer and stored at −20 °C until analysis.

Absolute quantification by qNGS

cfDNA samples containing QSs were prepared for NGS libraries using the QIAseq Targeted DNA Custom Panel Kit (QIAGEN, Courtaboeuf, France) with Single Primer Extension (SPE) technology. Library preparation followed manufacturer recommendations for cfDNA.

The NGS panel contained three primers that simultaneously target the QSs and corresponding reference loci **(Table 1)**.

Table 1. Sequencing primers targeting QSs and their matched reference regions.

NGS Primer	Sequence
QS1	GCCTAAATGCTCCACTTAAAAGCTAAAGATGACA
QS2	AAAAATGGGCGGAGGAGAGTAGTCTGAATT
QS3	CCAGTGTTGTGGGATATTAATGTGCATTACATAG

NGS Library Sequencing and Data Analysis

Sequencing of the prepared NGS libraries was carried out on a MiSeq system (Illumina, Évry-Courcouronnes, France). The resulting reads were processed through a bespoke analysis pipeline within CLC Genomics Workbench version 23 (QIAGEN).

In short, this workflow screened unaligned reads to detect the QS-specific insertion motif (GATTACAACA CGAGTTCGACCGCGT), thereby enabling discrimination between quality standards (QS) and cell-free DNA (cfDNA) originating from the biological sample. Both data sets were individually mapped to the human reference genome GRCh38 (hg38):

- QS reads: These were aligned precisely to their corresponding loci. The quantity of sequenced molecules for each QS was derived from its unique molecular identifier (UMI) count.
- Sample cfDNA reads: Following alignment, UMI-based quantification was applied to estimate the copy number per reference locus, and variant analysis was conducted to identify sequence alterations within cfDNA.

Because QS fragments were introduced at a predetermined concentration before extraction, the total cfDNA concentration (in genomic equivalents per mL of plasma) was computed using:

$$[\text{total cfDNA}] = \text{UMI}_{\text{ref}} \times \frac{[\text{QS}]}{\text{UMI}_{\text{QS}}} \quad (1)$$

Here, UMIref indicates the count of UMI-tagged reads mapped to the reference sequence, UMIQS represents the number of QS-specific UMIs, and [QS] corresponds to the known concentration of QS (copies/mL).
The mutant allele concentration (expressed as mutated copies/mL of plasma) was then determined using:

$$[\text{Variant}] = \text{VAF} \times [\text{total cfDNA}] \quad (2)$$

where VAF denotes the variant allele fraction, and [total cfDNA] is the calculated total cfDNA concentration (genomic equivalents/mL).
The final absolute measurement for each variant was taken as the median value of the results across all QS replicates.

Digital PCR quantification of nucleotide variants
To verify agreement with the qNGS findings, the variants EGFR exon 19 deletions, EGFR p.L858R (c.2573T > G), BRAF p.V600E (c.1799T > A), and NRAS p.Q61K (c.181C > A) were quantified through digital PCR (dPCR) performed on QS-enriched cfDNA samples.
Reactions were executed on the Naica Crystal Digital PCR platform (Stilla). Each 25 µL reaction mixture contained 1 µL of cfDNA template, PerfeCTa MultiPlex qPCR ToughMix (Quantabio, VWR International, Rosny-sous-Bois, France), 600 nM of mutation-specific primer pairs, and 200 nM of TaqMan probes. The samples were dispensed into Sapphire chips and amplified through 45 thermal cycles using the Geode cycler (Stilla). Fluorescent signals were recorded via the Prism3 reader and processed with Crystal Reader v4.0, while absolute quantification of each mutation (in mutated copies/µL of DNA) was determined by Crystal Miner v4.0 (Stilla).

Generation of artificial plasma samples
A pooled plasma sample obtained from healthy individuals was separated into eight aliquots (2 mL each). Each portion was supplemented with 200 ng of a reference cfDNA standard derived from cell lines (OncoSpan cfDNA, Catalog ID: HD833, Horizon Diagnostics, Cambridge, UK).
This OncoSpan material comprised 13 well-characterized somatic variants typical of multiple cancer types, all of which were detectable by the employed sequencing assay. The nominal concentrations were validated by the manufacturer **(Table 2)**. Each prepared aliquot was analyzed in triplicate, providing 24 data points per variant across all 13 loci.

Table 2. Variants included in the OncoSpan cfDNA reference, qNGS-determined concentrations in reconstructed samples, and analytical repeatability.

Variant	Absolute Concentration (copies/mL)	Coefficient of Variation
NRAS p.Q61K (p.Gln61Lys; c.181C>A)	1540.8	10.1%
CTNNB1 p.S33Y (p.Ser33Tyr; c.98C>A)	4006.1	10.4%
CTNNB1 p.S45del (p.Ser45del; c.133_135del)	1232.7	12.0%
PIK3CA p.E545K (p.Glu545Lys; c.1633G>A)	1109.4	14.5%
PIK3CA p.H1047R (p.His1047Arg; c.3140A>G)	2157.2	11.2%
KIT p.D816V (p.Asp816Val; c.2447A>T)	1232.7	13.4%
EGFR p.G719S (p.Gly719Ser; c.2155G>A)	3020.0	8.9%
EGFR p.E746_A750del (p.Glu746_Ala750del; c.2235_2249del)	246.5	25.1%
EGFR p.T790M (p.Thr790Met; c.2369C>T)	123.3	31.9%
EGFR p.L858R (p.Leu858Arg; c.2573T>G)	369.4	23.8%

BRAF p.V600E (p.Val600Glu; c.1799T>A)	1295.7	10.2%
KRAS p.G13D (p.Gly13Asp; c.38G>A)	1849.0	11.0%
KRAS p.G12D (p.Gly12Asp; c.35G>A)	739.6	17.2%

Results and Discussion

Validation of qNGS using artificially prepared plasma

To assess the analytical performance of the qNGS assay, we first examined synthetic plasma samples produced by supplementing healthy donor plasma with DNA reference materials.

Average sequencing coverage values were 1016X, 1112X, and 991X for QS1, QS2, and QS3, respectively (interquartile ranges: 820-1160X, 939-1250X, and 827-1112X). The mean sequencing depth at the corresponding reference sites was 1840X, 1302X, and 1415X, while targeted variants displayed an average depth of 2391X (Q1-Q3: 1903-2792X).

Across all 13 targeted alterations, qNGS provided accurate quantitative results with a correlation coefficient of $r^2 = 0.98$ and a regression slope of 0.81 **(Figure 2)**, indicating high linearity but a minor underestimation relative to expected concentrations.

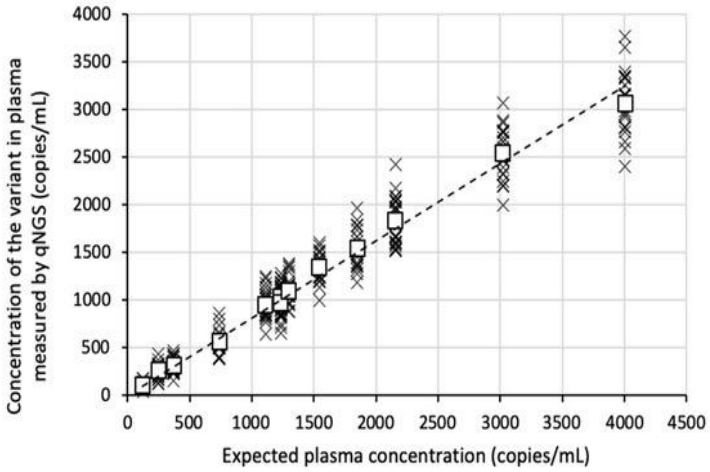

Figure 2. Evaluation of qNGS linearity in synthetic samples. Normal plasma was spiked with a DNA mixture containing 13 known variants detectable by the NGS panel. Eight replicates were generated and analyzed in triplicate using qNGS. Each point (cross) corresponds to an independent measurement, and white squares represent the mean concentrations. The regression line illustrates the linear fit.

The precision of the assay—expressed as repeatability **(Table 2)** and reproducibility **(Figure 3)**—improved as the variant copy number increased. The coefficient of variation (CV) decreased from 34.3% for the lowest-level variant (EGFR c.2369C > T, expected 123 copies/mL) to 10.6% for the highest-level variant (CTNNB1 c.98C > A, expected 4006 copies/mL).

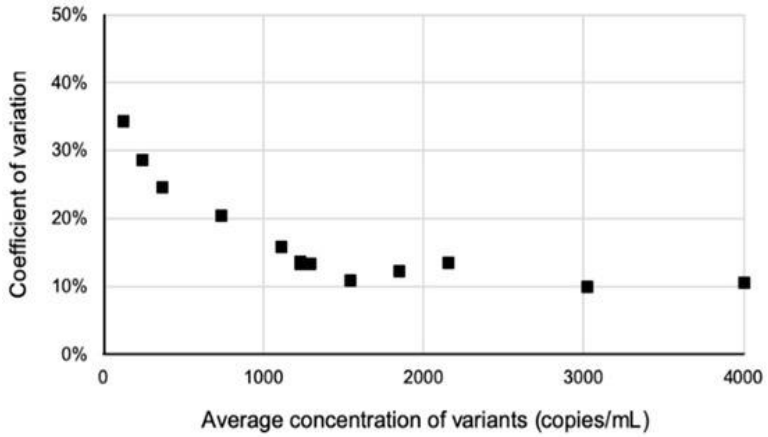

Figure 3. Relationship between ctDNA abundance and qNGS reproducibility. Plasma was enriched with the 13-variant standard detected by the NGS panel. Eight replicates were tested three times each. The variation coefficients for all variants were plotted against their concentrations.

Evaluation of qNGS in clinical plasma samples

We next applied qNGS to patient-derived plasma to measure circulating tumor DNA (ctDNA) levels. Positive control mixtures were created by combining plasma from three cancer patients carrying distinct variants: EGFR exon 19 deletion (c.2235_2249del), EGFR p.L858R (c.2573T > G), and BRAF p.V600E (c.1799T > A). Eight pooled plasma samples were analyzed using both qNGS and digital PCR (dPCR). A strong linear correlation was obtained between the two quantification methods ($r^2 = 0.981$); **(Figure 4)**.

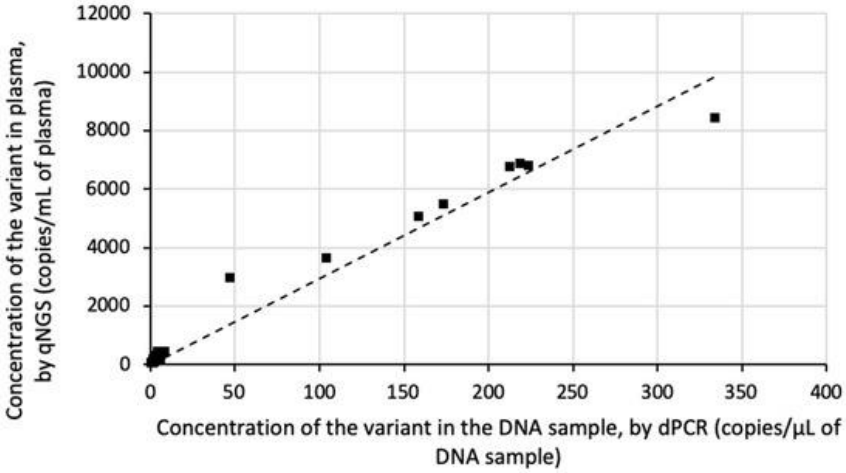

Figure 4. Correlation of qNGS and dPCR quantification in pooled NSCLC samples. Eight mixed plasma specimens were prepared by combining patient samples positive for EGFR exon 19 deletion, EGFR p.L858R, and BRAF p.V600E in various ratios. Variant levels were quantified by qNGS and dPCR, with linear regression showing excellent concordance.

Additionally, plasma from eight NSCLC patients known to harbor EGFR exon 19 deletions (confirmed in both tumor and cfDNA) was analyzed. Again, qNGS measurements closely matched dPCR values ($r^2 = 0.991$); **(Figure 5)**.

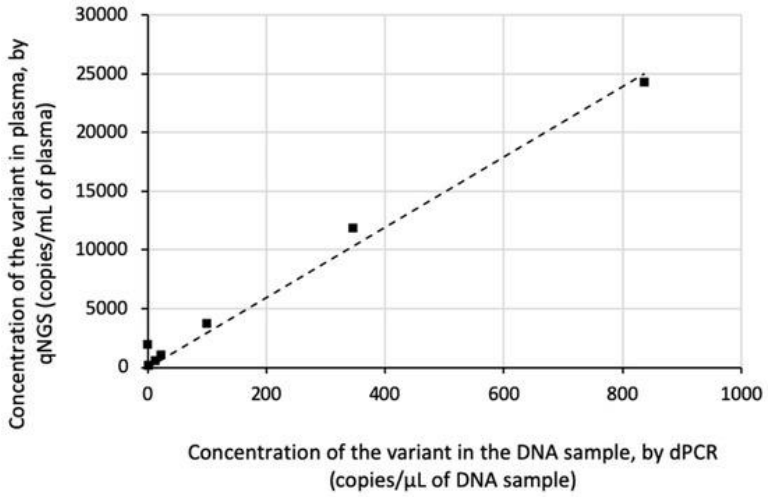

Figure 5. Comparison of qNGS and dPCR results for EGFR exon 19 deletions in NSCLC plasma. Eight cfDNA samples from NSCLC patients were tested by both platforms. Linear regression demonstrates strong consistency between the two methods.

Clinical implementation

To demonstrate qNGS utility in treatment monitoring, plasma samples collected before therapy (week 0) and after three weeks (week 3) were analyzed from four participants enrolled in the ELUCID trial (Early Assessment of Response to Treatment of Metastatic Lung Tumors Based on Circulating Tumor DNA, ClinicalTrials.gov ID NCT03926260).

This prospective, single-arm pilot study evaluates whether early variations in ctDNA concentration can anticipate imaging-based treatment responses in advanced or metastatic NSCLC, regardless of therapeutic regimen.

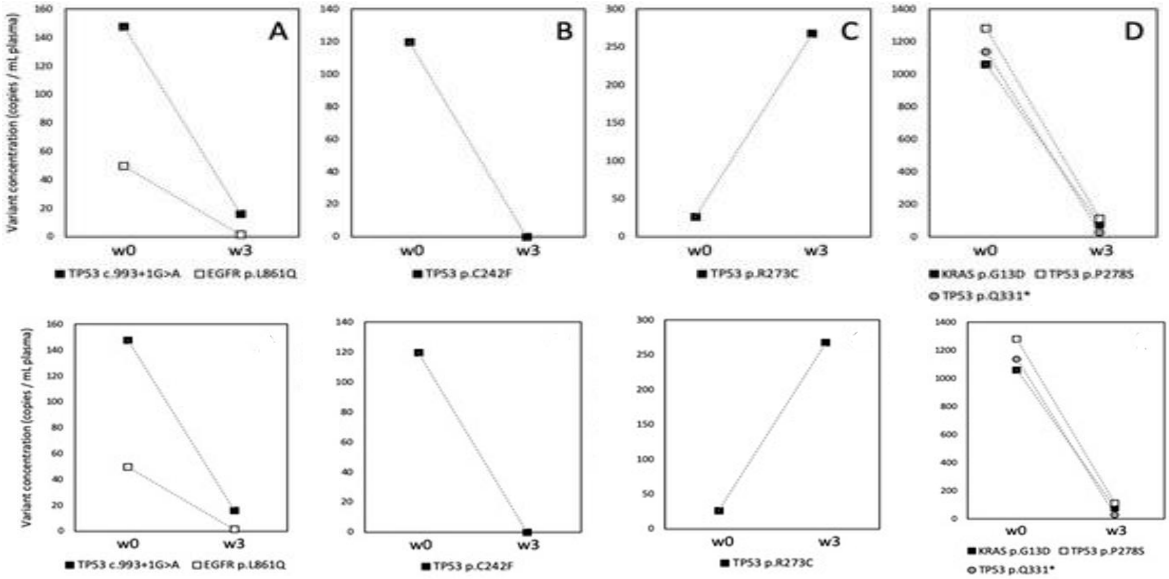

a) b) c) d)

Figure 6. Early ctDNA trends in NSCLC patients from the ELUCID study. Plasma was collected at week 0 (baseline) and week 3 after therapy initiation from four patients ((a-d), details above). The graph presents measured concentrations of each tumor-specific variant.

Patient 02-035: A 77-year-old male with a left upper-lobe carcinoma and brain plus nodal metastases carried EGFR p.L861Q (c.2582T > A) and TP53 (c.993 + 1G > A) mutations. Both were detected in baseline plasma (w0); **(Figure 6a)**. After osimertinib therapy, mutation levels fell markedly at week 3, aligning with a partial radiologic response.

Patient 02-021: A 71-year-old man with right lower-lobe cancer and lymph node metastasis exhibited an ALK rearrangement and TP53 p.C242F (c.725G > T) mutation. At baseline, only the TP53 variant appeared in cfDNA.

Following alectinib treatment, this mutation became undetectable at week 3 **(Figure 6b)**, concurrent with a partial response on CT imaging.

Patient 02-031: A 60-year-old female with left lower-lobe NSCLC and cutaneous and cerebral metastases harbored TP53 p.R273C (c.817C > T). The mutation was present at low levels pre-treatment **(Figure 6c)**. After three weeks of pembrolizumab, the ctDNA level increased roughly tenfold, followed by rapid clinical decline and death before the first imaging evaluation.

Patient 01-041: A 62-year-old male with a right lower-lobe tumor and metastases in lymph nodes and adrenal glands carried KRAS p.G13D (c.38G > A) and two TP53 mutations (p.Pro278Ser, c.832C > T and p.Gln331, c.991C > T*). All were present at baseline **(Figure 6d)**. Treatment combining carboplatin + pemetrexed chemotherapy and pembrolizumab immunotherapy resulted in a significant reduction of all mutation levels at week 3, consistent with partial tumor regression.

Most research examining the usefulness of circulating tumor DNA (ctDNA) in monitoring therapeutic response has centered on shifts in variant allele frequency (VAF). However, these analyses often rely on arbitrarily defined thresholds that vary among studies. For example, some investigations interpret a drop in VAF between baseline and follow-up as a sign of response [16], while others apply a ≥50% decline as a benchmark during targeted therapy [17], chemotherapy, or immunotherapy [18, 19]. In certain protocols, the complete disappearance of ctDNA is treated as the decisive endpoint [20]. Direct comparison between studies remains problematic since VAF values do not adjust for total cfDNA fluctuations that may occur independently of tumor changes.

To overcome these shortcomings, we designed a quantitative next-generation sequencing (qNGS) method for ctDNA variant detection. By integrating unique molecular identifiers (UMIs) with quantitative standards (QSs), this approach yields results that display a linear correlation with digital PCR (dPCR), the established reference technique for absolute variant quantification. When DNA-spiked plasma samples were tested, qNGS results showed a mean underestimation of 19% relative to theoretical values. This moderate deviation could stem from minor reconstitution inaccuracies or partial degradation of the OncoSpan reference DNA before lysis buffer addition.

Only a few protocols have been published that attempt to determine absolute variant concentrations using NGS. Hoerres and colleagues introduced a strategy employing synthetic oligonucleotides [21, 22] to standardize quantification of the Epstein-Barr virus (EBV) genome in plasma [23], reporting strong linearity when benchmarked against dPCR. In our workflow, UMIs enable the precise counting of distinct DNA molecules by eliminating PCR duplicate bias, whereas QSs provide normalization against a defined reference, ensuring consistent quantification. Importantly, QS design must correspond to both the library preparation chemistry and the sequencing panel. Here, three QSs were crafted to mirror three reference loci covered by our panel and specifically optimized for the single primer enrichment (SPE)-based preparation, which amplifies targets using one primer per region. Should other primer sets be employed, the QS sequences must be reconfigured accordingly. Furthermore, adopting a larger number of QSs would likely enhance the accuracy of genomic equivalent calculations, leading to improved precision in variant quantification.

One potential source of inaccuracy arises from somatic copy number variations (CNVs) affecting genes of interest. The qNGS model assumes each genome in cfDNA harbors two copies of every target gene. When a locus undergoes amplification, this assumption fails, resulting in underestimated variant concentrations. From a clinical standpoint, gene amplification is challenging for any quantification method, as it disrupts the proportionality between ctDNA level and actual tumor burden, potentially leading to misguided clinical interpretations. Therefore, identifying CNVs in the primary tumor whenever feasible is essential to avoid using amplified alleles for ctDNA quantification. Employing variants from separate genes is also advisable to ensure a more reliable representation of overall ctDNA levels.

The validation experiments in this study were performed under controlled laboratory conditions. Using our current sequencing depth and bioinformatics parameters, the assay reliably detects mutations with allele frequencies between 0.5% and 1%. In OncoSpan standard samples, observed VAFs ranged from 0.8% (EGFR p.T790M) to 22.4% (CTNNB1 p.S33Y), establishing the effective quantitative range for this approach. Achieving greater sensitivity would require increasing DNA input, enhancing sequencing depth, and optimizing analytical pipelines [24-26]. Further development is needed to extend detection toward low-abundance variants.

Quantitative NGS has considerable promise for improving ctDNA-based disease monitoring, offering a means to evaluate tumor dynamics without interference from non-tumor cfDNA changes [8-10]. A major advantage over targeted assays like dPCR is that qNGS does not depend on prior knowledge of a tumor's specific mutations,

provided that the panel design is sufficiently comprehensive. The ability to quantify multiple variants simultaneously is particularly valuable, since focusing on a single alteration risks tracking a subclonal population that may not represent the overall tumor [27]. By integrating several somatic variants, qNGS delivers a more holistic picture of tumor burden and can reveal emerging resistance-associated mutations.

The case studies from the ELUCID trial illustrate these benefits. In those patients, tumor genotyping had been performed beforehand, facilitating assay validation. Nevertheless, the interpretation of ctDNA kinetics would likely have been similar even in the absence of prior genotype data, underscoring the flexibility and clinical utility of the quantitative NGS framework.

Conclusion

This study presents a novel approach for absolute ctDNA quantification via NGS, effectively mitigating distortions caused by variations in non-tumor cfDNA. The proof-of-concept evaluation, conducted on a small patient cohort, highlights the method's clinical potential. The same workflow is currently applied to plasma samples from the complete ELUCID cohort (n = 100) to determine whether early ctDNA kinetics can reliably predict therapeutic response across diverse treatment types.

By eliminating dependence on individualized tumor genotypes, this qNGS strategy provides a standardized and broadly applicable solution for ctDNA analysis. Its ability to quantify multiple variants in parallel offers a more comprehensive and non-invasive method for tumor monitoring and treatment assessment, paving the way for improved clinical decision-making and personalized patient management.

Acknowledgments: None

Conflict of Interest: None

Financial Support: None

Ethics Statement: None

References

1. Alexander EM, Miller HA, Egger ME, Smith ML, Yaddanapudi K, Linder MW. The correlation between plasma circulating tumor DNA and radiographic tumor burden. J Mol Diagn. 2024;26(11):952–61.
2. Taus A, Camacho L, Rocha P, Hardy-Werbin M, Pijuan L, Piquer G, et al. Dynamics of EGFR mutation load in plasma for prediction of treatment response and disease progression in patients with EGFR-mutant lung adenocarcinoma. Clin Lung Cancer. 2018;19(5):387–94.e2.
3. Urbini M, Marisi G, Azzali I, Bartolini G, Chiadini E, Capelli L, et al. Dynamic monitoring of circulating tumor DNA in patients with metastatic colorectal cancer. JCO Precis Oncol. 2023;7:e2200694.
4. Herbreteau G, Vallée A, Knol A-C, Théoleyre S, Quéreux G, Varey E, et al. Circulating tumor DNA early kinetics predict response of metastatic melanoma to anti-PD1 immunotherapy: Validation study. Cancers. 2021;13(8):1826.
5. Zhang Y, Yao Y, Xu Y, Li L, Gong Y, Zhang K, et al. Pan-cancer circulating tumor DNA detection in over 10,000 Chinese patients. Nat Commun. 2021;12(1):11.
6. Li L, Wang Y, Shi W, Zhu M, Liu Z, Luo N, et al. Serial ultra-deep sequencing of circulating tumor DNA reveals the clonal evolution in non-small cell lung cancer patients treated with anti-PD1 immunotherapy. Cancer Med. 2019;8(20):7669–78.
7. Hua G, Zhang X, Zhang M, Wang Q, Chen X, Yu R, et al. Real-world circulating tumor DNA analysis depicts resistance mechanism and clonal evolution in ALK inhibitor–treated lung adenocarcinoma patients. ESMO Open. 2022;7:100337.
8. Vittori LN, Tarozzi A, Latessa PM. Circulating cell-free DNA in physical activities. Methods Mol Biol. 2019;1909:183–97.
9. Shin C, Kim JK, Kim JH, Jung KH, Cho KJ, Lee CK, et al. Increased cell-free DNA concentrations in patients with obstructive sleep apnea. Psychiatry Clin Neurosci. 2008;62(6):721–7.

10. Dwivedi DJ, Toltl LJ, Swystun LL, Pogue J, Liaw KL, Weitz JI, et al. Prognostic utility and characterization of cell-free DNA in patients with severe sepsis. Crit Care. 2012;16(6):R151.
11. Lo YM, Rainer TH, Chan LY, Hjelm NM, Cocks RA. Plasma DNA as a prognostic marker in trauma patients. Clin Chem. 2000;46(2):319–23.
12. Galeazzi M, Morozzi G, Piccini M, Chen J, Bellisai F, Fineschi S, et al. Dosage and characterization of circulating DNA: Present usage and possible applications in systemic autoimmune disorders. Autoimmun Rev. 2003;2(1):50–5.
13. Galant N, Nicos M, Kuznar-Kaminska B, Krawczyk P. Variant allele frequency analysis of circulating tumor DNA as a promising tool in assessing the effectiveness of treatment in non–small cell lung carcinoma patients. Cancers. 2024;16(2):782.
14. Islam S, Zeisel A, Joost S, La Manno G, Zajac P, Kasper M, et al. Quantitative single-cell RNA-seq with unique molecular identifiers. Nat Methods. 2014;11(2):163–6.
15. Jiang P, Chan CW, Chan KC, Cheng SH, Wong J, Wong VW, et al. Lengthening and shortening of plasma DNA in hepatocellular carcinoma patients. Proc Natl Acad Sci U S A. 2015;112(11):E1317–25.
16. Ernst SM, van Marion R, Atmodimedjo PN, de Jonge E, Mathijssen RHJ, Paats MS, et al. Clinical utility of circulating tumor DNA in patients with advanced KRAS(G12C)-mutated NSCLC treated with sotorasib. J Thorac Oncol. 2024;19(7):995–1006.
17. Soo RA, Martini JF, van der Wekken AJ, Teraoka S, Ferrara R, Shaw AT, et al. Early circulating tumor DNA dynamics and efficacy of lorlatinib in patients with treatment-naive, advanced, ALK-positive NSCLC. J Thorac Oncol. 2023;18(12):1568–80.
18. Vega DM, Nishimura KK, Zariffa N, Thompson JC, Hoering A, Cilento V, et al. Changes in circulating tumor DNA reflect clinical benefit across multiple studies of patients with non–small-cell lung cancer treated with immune checkpoint inhibitors. JCO Precis Oncol. 2022;6:e2100372.
19. Jun S, Shukla NA, Durm G, Hui AB, Cao S, Ganti AK, et al. Analysis of circulating tumor DNA predicts outcomes of short-course consolidation immunotherapy in unresectable stage III NSCLC. J Thorac Oncol. 2024;19(8):1427–37.
20. Pan Y, Zhang JT, Gao X, Chen ZY, Yan B, Tan PX, et al. Dynamic circulating tumor DNA during chemoradiotherapy predicts clinical outcomes for locally advanced non-small cell lung cancer patients. Cancer Cell. 2023;41(12):1763–73.e4.
21. Gulley ML, Elmore S, Gupta GP, Kumar S, Egleston M, Hoskins IJ, et al. Use of spiked normalizers to more precisely quantify tumor markers and viral genomes by massive parallel sequencing of plasma DNA. J Mol Diagn. 2020;22(3):437–46.
22. Zook JM, Samarov D, McDaniel J, Sen SK, Salit M. Synthetic spike-in standards improve run-specific systematic error analysis for DNA and RNA sequencing. PLoS ONE. 2012;7(7):e41356.
23. Hoerres D, Dai Q, Elmore S, Sheth S, Gupta GP, Kumar S, et al. Calibration of cell-free DNA measurements by next-generation sequencing. Am J Clin Pathol. 2023;160(3):314–21.
24. Larson NB, Oberg AL, Adjei AA, Wang L. A clinician's guide to bioinformatics for next-generation sequencing. J Thorac Oncol. 2023;18(2):143–57.
25. Tebar-Martinez R, Martin-Arana J, Gimeno-Valiente F, Tarazona N, Rentero-Garrido P, Cervantes A. Strategies for improving detection of circulating tumor DNA using next generation sequencing. Cancer Treat Rev. 2023;119:102595.
26. Li W, Huang X, Patel R, Schleifman E, Fu S, Shames DS, Zhang J. Analytical evaluation of circulating tumor DNA sequencing assays. Sci Rep. 2024;14:4973.
27. Abbosh C, Frankell AM, Harrison T, Kisistok J, Garnett A, Johnson L, et al. Tracking early lung cancer metastatic dissemination in TRACERx using ctDNA. Nature. 2023;616(7959):553–62.